Figure S1

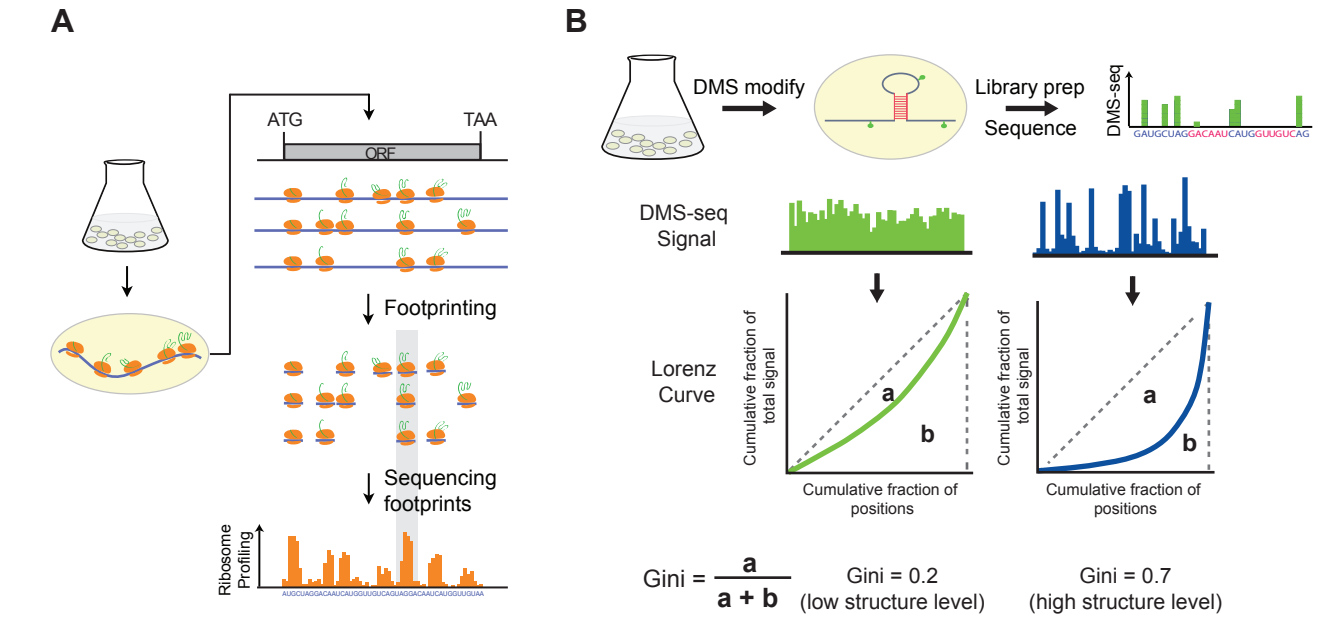
A
ATG
TAA
ORF
Footprinting
Sequencing footprints
Ribosome Profiling
B
DMS modify
Library prep
Sequence
DMS-seq
DMS-seq Signal
Lorenz Curve
Cumulative fraction of total signal
Cumulative fraction of positions
a
b
Gini = a / (a + b)
Gini = 0.2 (low structure level)
Gini = 0.7 (high structure level)

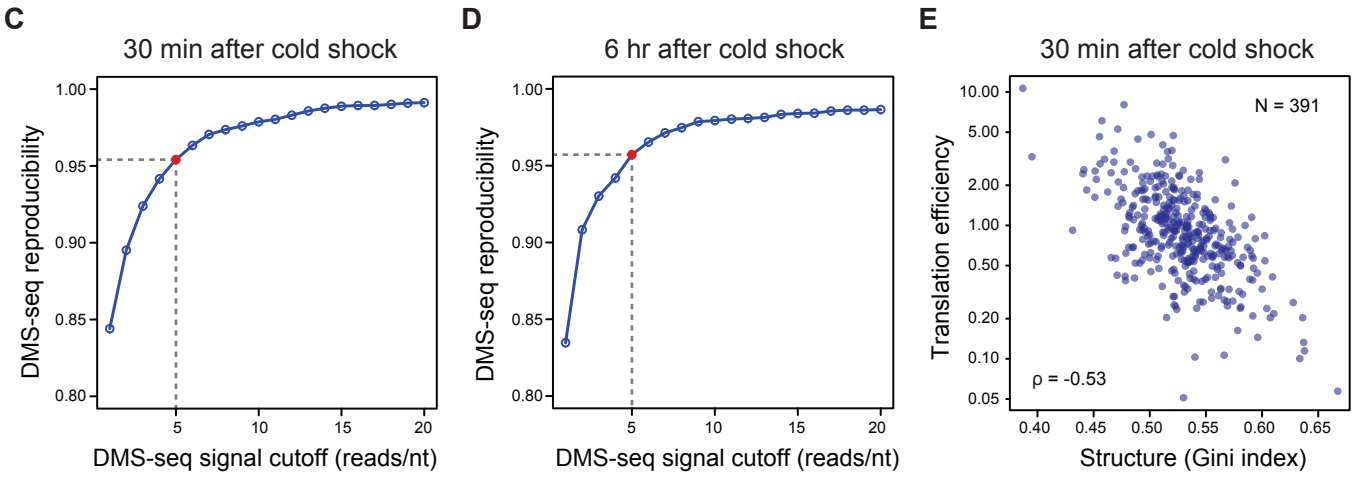
C
30 min after cold shock
DMS-seq reproducibility
DMS-seq signal cutoff (reads/nt)
D
6 hr after cold shock
DMS-seq reproducibility
DMS-seq signal cutoff (reads/nt)
E
30 min after cold shock
Translation efficiency
N = 391
ρ = -0.53
Structure (Gini index)

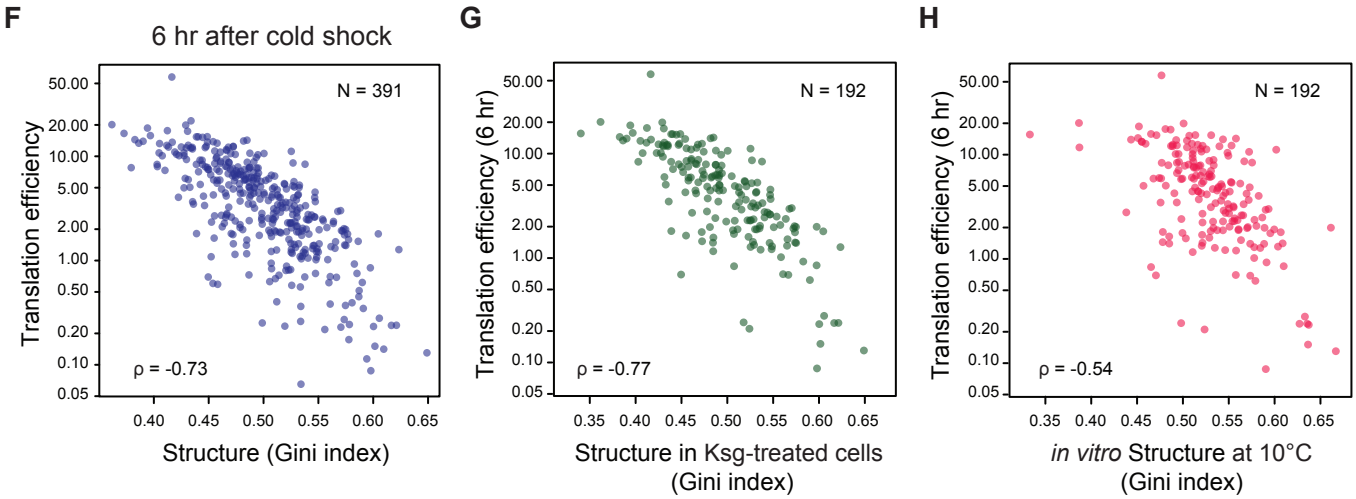
F
6 hr after cold shock
Translation efficiency
N = 391
ρ = -0.73
Structure (Gini index)
G
Translation efficiency (6 hr)
N = 192
ρ = -0.77
Structure in Ksg-treated cells (Gini index)
H
Translation efficiency (6 hr)
N = 192
ρ = -0.54
in vitro Structure at 10°C (Gini index)

Figure S1, related to Figure 1: ORF-wide mRNA structure level and translation efficiency are highly correlated during the acclimation phase after cold shock

(A) Schematic for using ribosome profiling to quantify genome-wide translation rate. The overall rate of protein production is determined from the average ribosome footprint density of an ORF (number of footprints/ unit length of ORF). Orange: ribosomes; blue line: mRNA.

(B) Schematic for genome-wide probing of mRNA secondary structures using DMS-seq and calculation of Gini index to quantify mRNA structure level of an ORF as in (Burkhardt et al., 2017). For a region of mRNA, the cumulative fraction of the total DMS-seq signal is plotted against the cumulative fraction of the total number of positions as a Lorenz Curve. The extent to which the curve sags below the diagonal line indicates the degree of inequality of distribution, which is quantified by the Gini index defined as the ratio of the area between the diagonal line and the Lorenz Curve (a) to the total area below the diagonal line (a + b). A high Gini index indicates high level of mRNA structure, and vice versa.

(C, D) Plot showing the effect of DMS-seq read coverage on the reproducibility of structure determination for WT cells collected at 30 min (C) or 6 hr (D) after shift to 10˚C. Reproducibility is measured by the median of Pearson's R values calculated by comparing two replicates of DMS-seq signals within the first 200nt of ORFs that pass the DMS-seq depth cutoff indicated in X-axis. A read coverage of ~5 reads/nucleotide is sufficient for reproducible structure determination.

(E, F) Plot comparing the Gini indices of ORFs calculated from *in vivo* DMS-seq to their translation efficiency at 30 min (E) or 6 hr (F) after cold shock. Genes with relatively constant mRNA across the ORF and a mean DMS-seq signal of ≥ 5 reads/nt in both

samples were selected (N = 391). Spearman's rank order correlation coefficient (ρ) is indicated.

(G, H) Plot comparing the Gini indices of ORFs calculated from *in vivo* DMS-seq in kasugamycin-treated cells (G) or from *in vitro* DMS-seq at 10˚C (H) to their translation efficiency at 6 hr after cold shock. Spearman's rank order correlation coefficient (ρ) is indicated. Genes with relatively constant mRNA across the ORF and a mean DMS-seq signal of ≥ 5 reads/nt in both samples were selected (N = 192). The translation initiation inhibitor, kasugamycin, was added to a final concentration of 10 mg/mL after 6 hr at 10°C for 40 min prior to DMS modification.

Figure S2

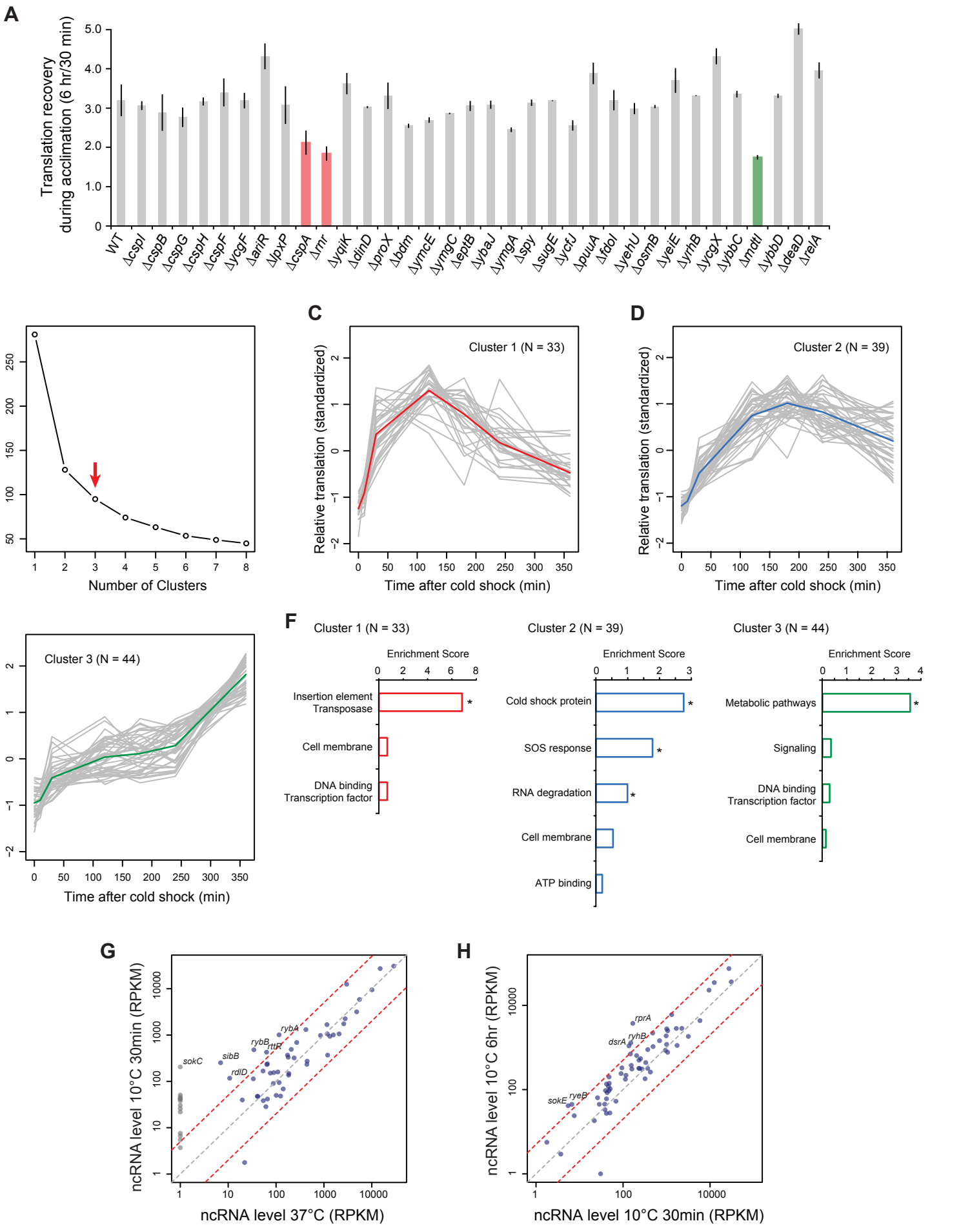
A
Translation recovery during acclimation (6 hr/30 min)
WT
ΔcspI
ΔcspB
ΔcspG
ΔcspH
ΔcspF
ΔycgF
ΔariR
ΔlpxP
ΔcspA
Δrnr
ΔyqiK
ΔdinD
ΔproX
Δbdm
ΔymcE
ΔymgC
ΔeptB
ΔybaJ
ΔymgA
Δspy
ΔsugE
ΔycfJ
ΔpuuA
Δfdol
ΔyehU
ΔosmB
ΔyeiE
ΔyrhB
ΔycgX
ΔybbC
Δmdtl
ΔybbD
ΔdeaD
ΔrelA
B
Within groups sum of squares
Number of Clusters
C
Cluster 1 (N = 33)
Relative translation (standardized)
Time after cold shock (min)
D
Cluster 2 (N = 39)
Relative translation (standardized)
Time after cold shock (min)
E
Cluster 3 (N = 44)
Relative translation (standardized)
Time after cold shock (min)
F
Cluster 1 (N = 33)
Enrichment Score
Insertion element Transposase
Cell membrane
DNA binding Transcription factor
Cluster 2 (N = 39)
Enrichment Score
Cold shock protein
SOS response
RNA degradation
Cell membrane
ATP binding
Cluster 3 (N = 44)
Enrichment Score
Metabolic pathways
Signaling
DNA binding Transcription factor
Cell membrane
G
ncRNA level 10°C 30min (RPKM)
ncRNA level 37°C (RPKM)
sokC
sibB
rdlD
rybB
rttR
rybA
H
ncRNA level 10°C 6hr (RPKM)
ncRNA level 10°C 30min (RPKM)
sokE
ryeB
dsrA
ryhB
rprA

Figure S2, related to Figure 2: Cold shock-induced genes and their effect on translation recovery during the acclimation phase

(A) Translation recovery of WT cells and deletion mutants of each of the most upregulated genes upon cold shock. Translation recovery was measured by comparing the ^{35}S-methionine incorporation rate at 6 hr vs 30 min after cold shock (see Methods). Three deletion alleles with strong defect in translation recovery are highlighted: *cspA* (red), *rnr* (red) and *mdtI* (green). We did not consider *mdtI* further, because most of its apparent reduction in recovery of protein synthesis comes from an increase in protein synthesis at 30 min relative to WT cells, rather than reduced protein synthesis at 6 hr. *mdtI* encodes for the membrane subunit of a heterodimeric spermidine efflux transporter. Spermidine accumulates and inhibits protein translation at low temperature by replacing the ribosome-bound Mg^{2+} (Limsuwun and Jones, 2000), so it is likely that high level of spermidine in *mdtI* mutant is changing the cellular translation after cold shock. Three other deletion alleles are significantly but mildly defective in translation recovery: *bdm*, a member of the Rcs regulon that is involved in biofilm formation (Francez-charlot et al., 2005); *ymgA*, which was reported to involve in biofilm formation and induced at low temperature (White-Ziegler et al., 2008); and *ycfJ*, whose function is still unknown. Although not highly induced, *deaD* and *relA* were included because of their potential impact on cold shock response.

(B-E) The 116 cold-induced genes (> 2-fold upregulated) are clustered into 3 groups using the k-means method based on their relative expression pattern during acclimation phase (see also Table S3). A plot of the within groups sum of squares by number of clusters extracted was shown in (B). We chose to group the data into 3 clusters, because this is the lowest number of clusters immediately after the large drop in the sum of squares, indicating that we had captured most of the diversity of the dataset. The

relative expression level of each gene was calculated from the number of ribosome footprint reads mapped to the ORF normalized to the number of total reads from ribosome profiling. The standardized relative expression levels of genes within 3 different clusters were plotted (as grey lines in C-E), with the mean curve colored in red, blue and green, respectively.

(F) Gene functional classification of 3 different clusters. DAVID enrichment scores were shown, with asterisks indicating significance ($p < 0.05$).

(G) Scatter plot comparing non-coding RNA amounts (RPKM) at 37°C versus 30 min after cold shock. Grey dash line: y = x; red dash lines: 5-fold up- or down-regulated. Grey dots indicate that the ncRNA level at 37°C is below detection limit (assigned as 1 only for plotting). Some sRNAs upregulated > 5-fold are highlighted (see also Table S4).

(H) Scatter plot comparing non-coding RNA amounts (RPKM) 30 min versus 6 hr after cold shock. Grey dash line: y = x; red dash lines: 5-fold up- or down-regulated. Some sRNAs upregulated > 5-fold are highlighted (see also Table S4).

Figure S3

A

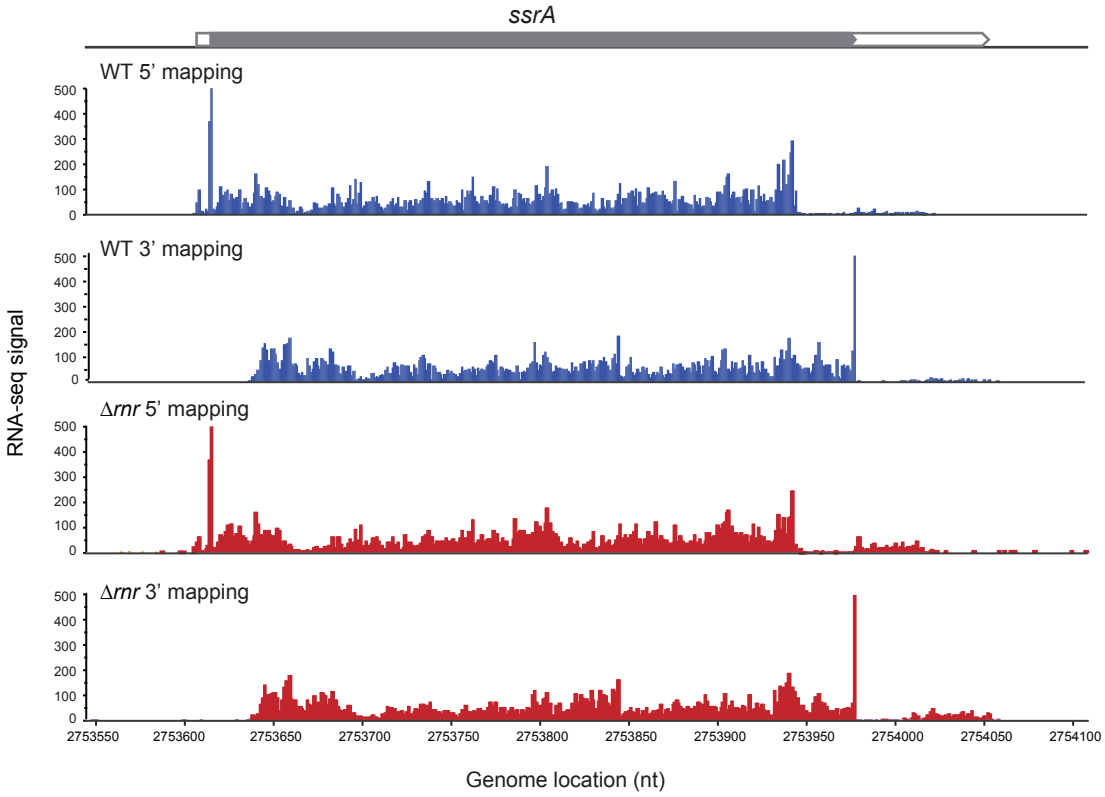

B

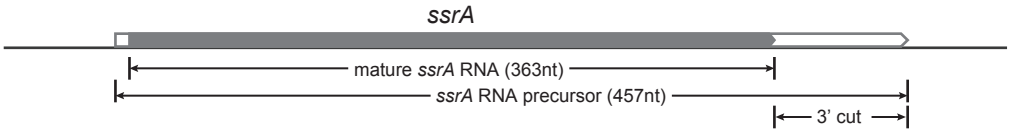

$$\text{"unprocessed" ratio} = \frac{\text{mean RNA-seq signal within "3-cut" region}}{\text{mean RNA-seq signal within "mature RNA" region}}$$

Time at 10˚C	20 min	4 hr	8 hr
WT 5' mapping	5.4%	6.0%	3.6%
WT 3' mapping	6.6%	7.3%	4.6%
Δ*rnr* 5' mapping	12.5%	20.6%	32.3%
Δ*rnr* 3' mapping	13.8%	22.4%	33.6%

Figure S3, related to Figure 3: Effect of RNase R on *ssrA* RNA processing upon cold shock

(A) RNA-seq signal mapped to *ssrA* RNA in WT or Δ*rnr* cells at 4 hr after cold shock. Sequencing reads were mapped either by their 5' ends (5' mapping) or 3' ends (3' mapping). RNA-seq signals were adjusted based on the total RNA-seq reads, so that different samples are directly comparable. Top: a diagram of *ssrA* RNA processing, with the RNA precursor (457 nt) shown in white and the mature *ssrA* RNA (363 nt) shown in grey.

(B) Ratio of "unprocessed" mRNA (within "3' cut region") level against the mature *ssrA* RNA level of WT and Δ*rnr* cells at various time points after cold shock, calculated from 5' or 3' mapped RNA-seq data. The higher "unprocessed" ratio in Δ*rnr* cells relative to WT cells suggests defect in endonuclease cleavage at 3' end of mature RNA, defect in exonuclease cleavage within the 3' cut fragment, or both. However, the total level of processed and the pre-processed *ssrA* RNA is not strongly affected by deletion of *rnr*, and most of the *ssrA* RNA is in the processed form.

Figure S4

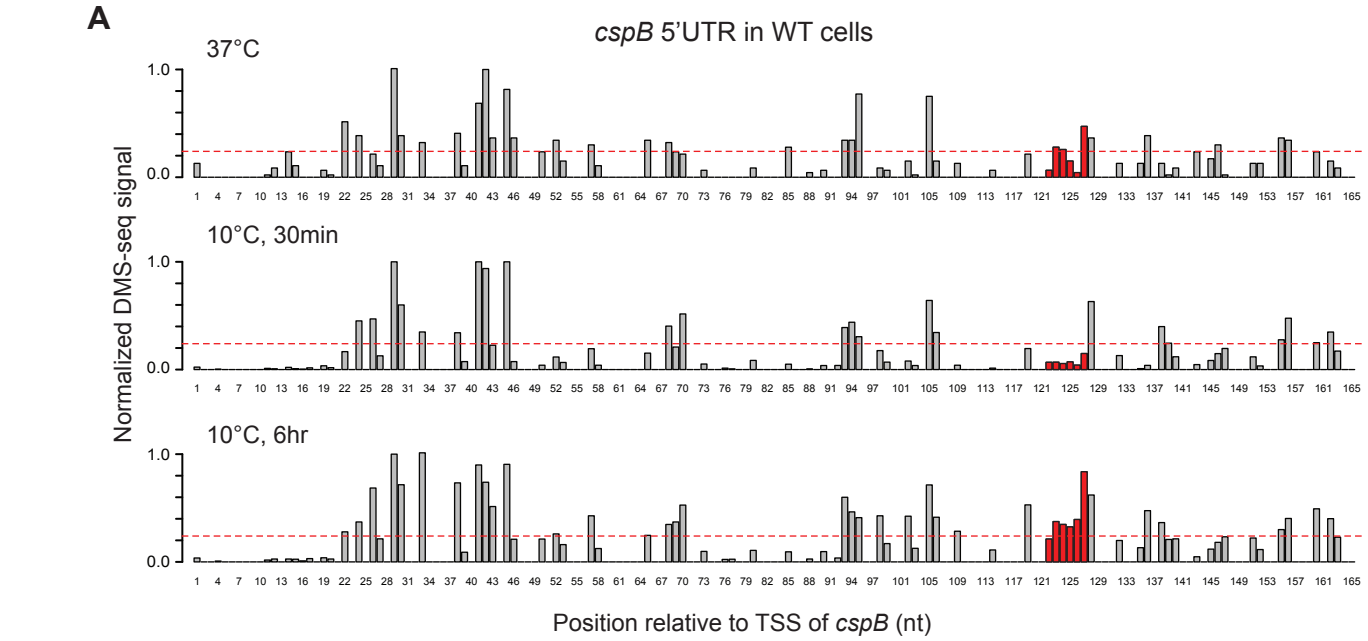
A
cspB 5'UTR in WT cells
37°C
10°C, 30min
10°C, 6hr
Normalized DMS-seq signal
Position relative to TSS of cspB (nt)

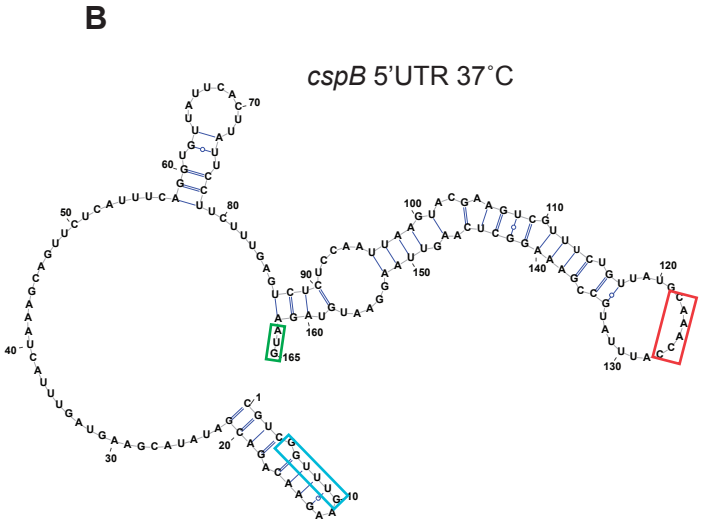
B
cspB 5'UTR 37˚C

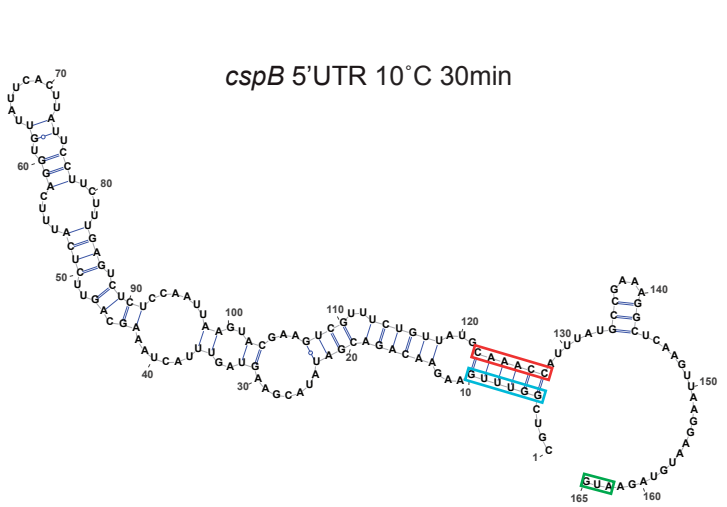
C
cspB 5'UTR 10˚C 30min

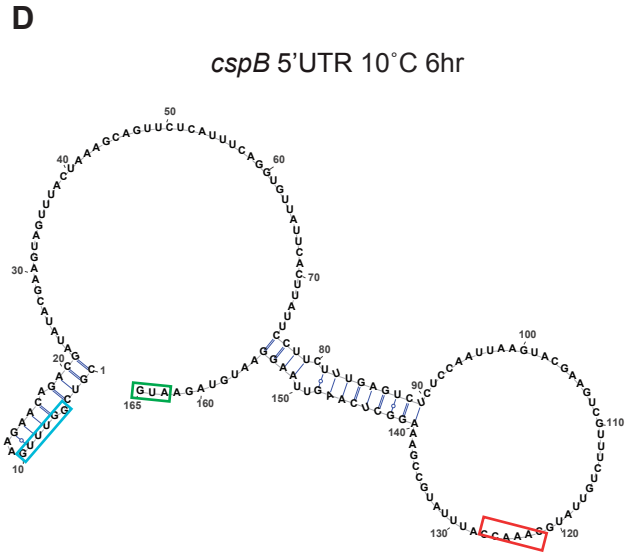
D
cspB 5'UTR 10˚C 6hr

Figure S4, related to Figure 5: The 5'UTR of *cspB* mRNA changes in structure during acclimation

(A) The normalized *in vivo* DMS-seq signal of A/C bases within *cspB* 5'UTR in WT cells at 37°C (top), 30 min after cold shock (middle) and 6 hr after cold shock (bottom). DMS-seq signals were pooled from 3 different replicates, and normalized to the maximum signal within *cspB* message after removing outliers by 98% Winsorisation (see Methods). The red dash line represents the signal cutoff (0.24), above which we assigned the bases to be non-base-paired. The region highlighted in red has long-range interactions with the "cold box" element at 10°C.

(B-D) The predicted structure of the *cspB* 5' UTR at (B) 37°C, (C) 30 min or (D) 6 hr after cold shock. Structure predictions were generated by constraining a minimum free-energy prediction with *in vivo* DMS-seq measurements. The start codon of *cspB* (green), the conserved "cold box" element (blue) and its long-range interaction region at 10°C (red) are highlighted in different structures. Due to the low expression level of *cspB* at 37°C (mean DMS-seq signal < 5 reads/nt), this structure model (B) is less reliable.

Figure S5

A

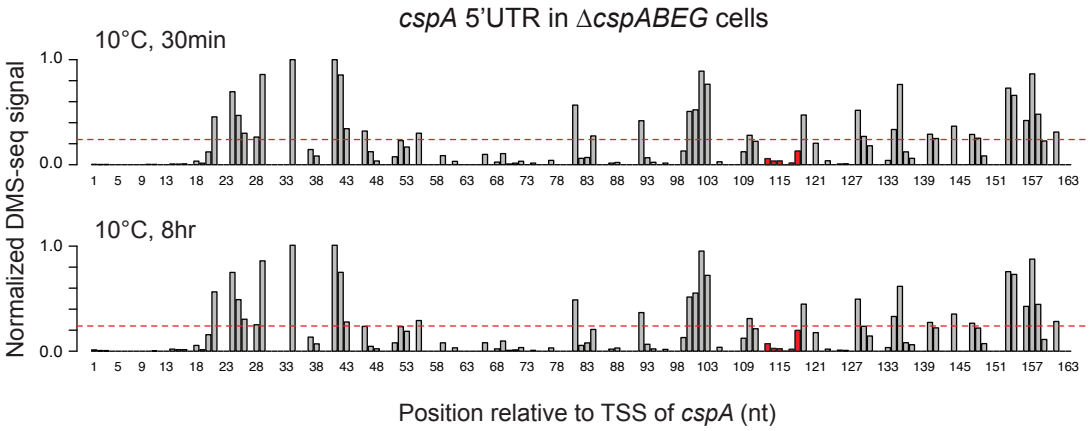
cspA 5'UTR in ΔcspABEG cells
10°C, 30min
10°C, 8hr
Normalized DMS-seq signal
1.0
0.0
1 5 9 13 18 23 28 33 38 43 48 53 58 63 68 73 78 83 88 93 98 103 109 115 121 127 133 139 145 151 157 163
Position relative to TSS of cspA (nt)

B

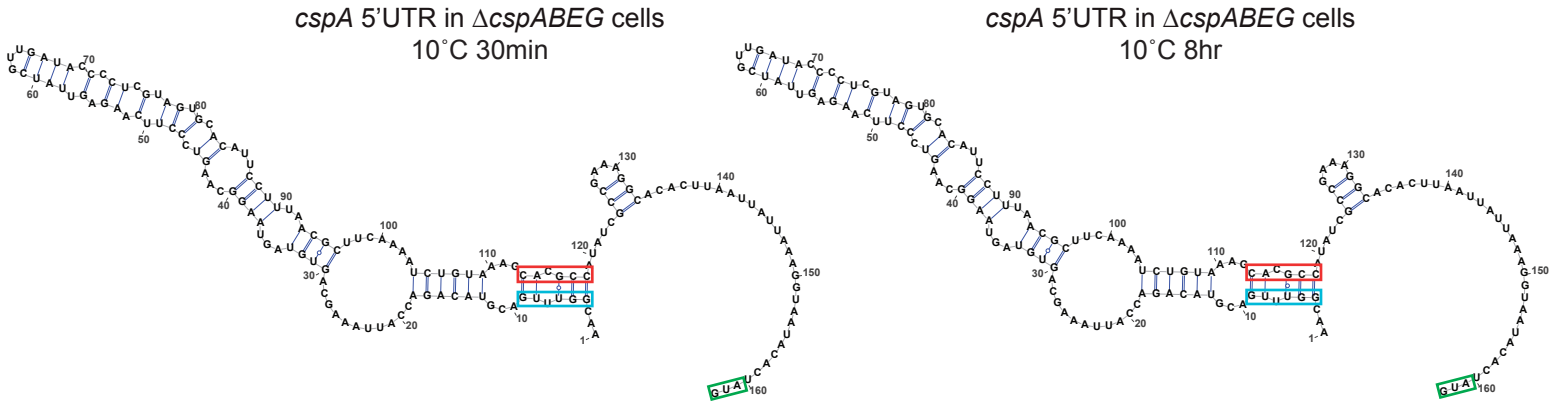
cspA 5'UTR in ΔcspABEG cells
10˚C 30min
cspA 5'UTR in ΔcspABEG cells
10˚C 8hr

Figure S5, related to Figure 5: The structure of *cspA* 5'UTR does not change in Δ*cspABEG* cells during acclimation

(A) The normalized *in vivo* DMS-seq signal of A/C bases within *cspA* 5'UTR in Δ*cspABEG* cells at 30 min or 8 hr after cold shock, shown as in Figure S4A. DMS-seq signals were scaled relative to the most reactive position in the 5'UTR of *cspA* after removing outliers by 98% Winsorisation.

(B) The predicted structure of the *cspA* 5' UTR in Δ*cspABEG* cells at 30 min or 8 hr after cold shock. Structure predictions were generated by constraining a minimum free-energy prediction with *in vivo* DMS-seq measurements. The start codon of *cspA* (green), the conserved "cold box" element (blue) and its long-range interaction region at 10°C (red) are highlighted in different structures.

A

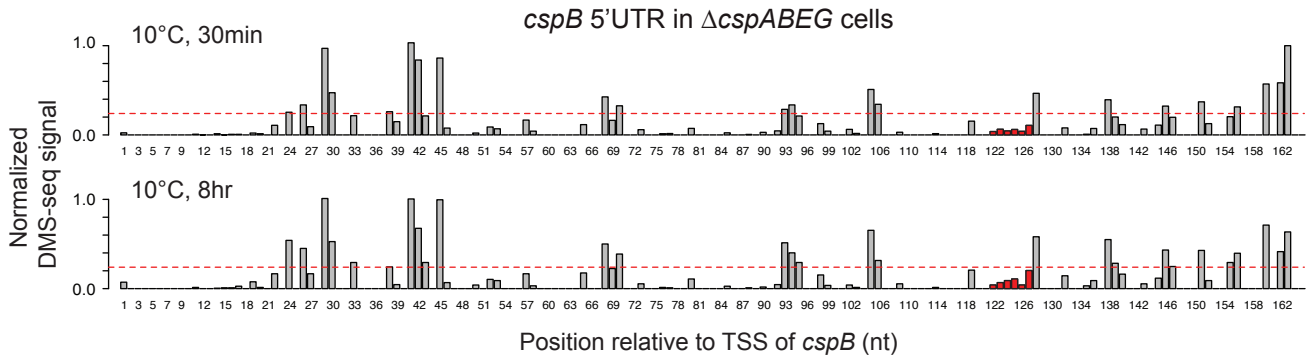
cspB 5'UTR in ΔcspABEG cells
10°C, 30min
10°C, 8hr
Normalized DMS-seq signal
1.0
0.0
Position relative to TSS of cspB (nt)

B

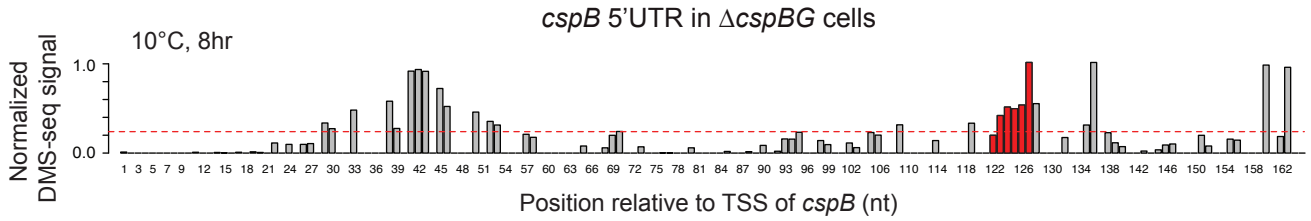
cspB 5'UTR in ΔcspBG cells
10°C, 8hr
Normalized DMS-seq signal
1.0
0.0
Position relative to TSS of cspB (nt)

C

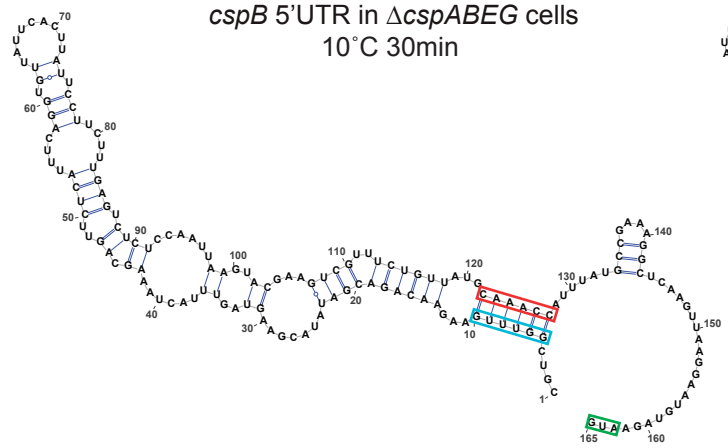
cspB 5'UTR in ΔcspABEG cells
10˚C 30min

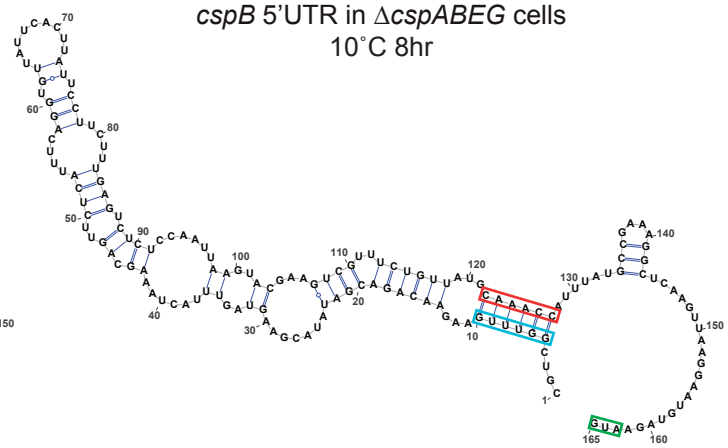
cspB 5'UTR in ΔcspABEG cells
10˚C 8hr

D

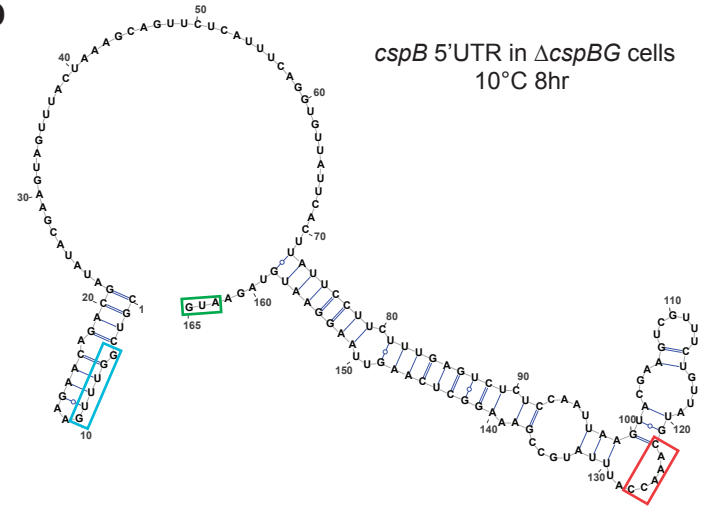
cspB 5'UTR in ΔcspBG cells
10˚C 8hr

Figure S6, related to Figure 5: The structure of *cspB* 5'UTR does not change in Δ*cspABEG* cells during acclimation

(A) The normalized *in vivo* DMS-seq signal of A/C bases within *cspB* 5'UTR in Δ*cspABEG* cells at 30 min or 8 hr after cold shock, shown as in Figure S5A. DMS-seq signals were scaled relative to the most reactive position in the 5'UTR of *cspB* after removing outliers by 98% Winsorisation.

(B) The normalized *in vivo* DMS-seq signal of A/C bases within *cspB* 5'UTR in Δ*cspBG* cells at 8 hr after cold shock, as in (A).

(C) The predicted structure of the *cspB* 5' UTR in Δ*cspABEG* cells at 30 min or 8 hr after cold shock.

(D) The predicted structure of the *cspB* 5' UTR in Δ*cspBG* cells at 8 hr after cold shock.

Figure S7

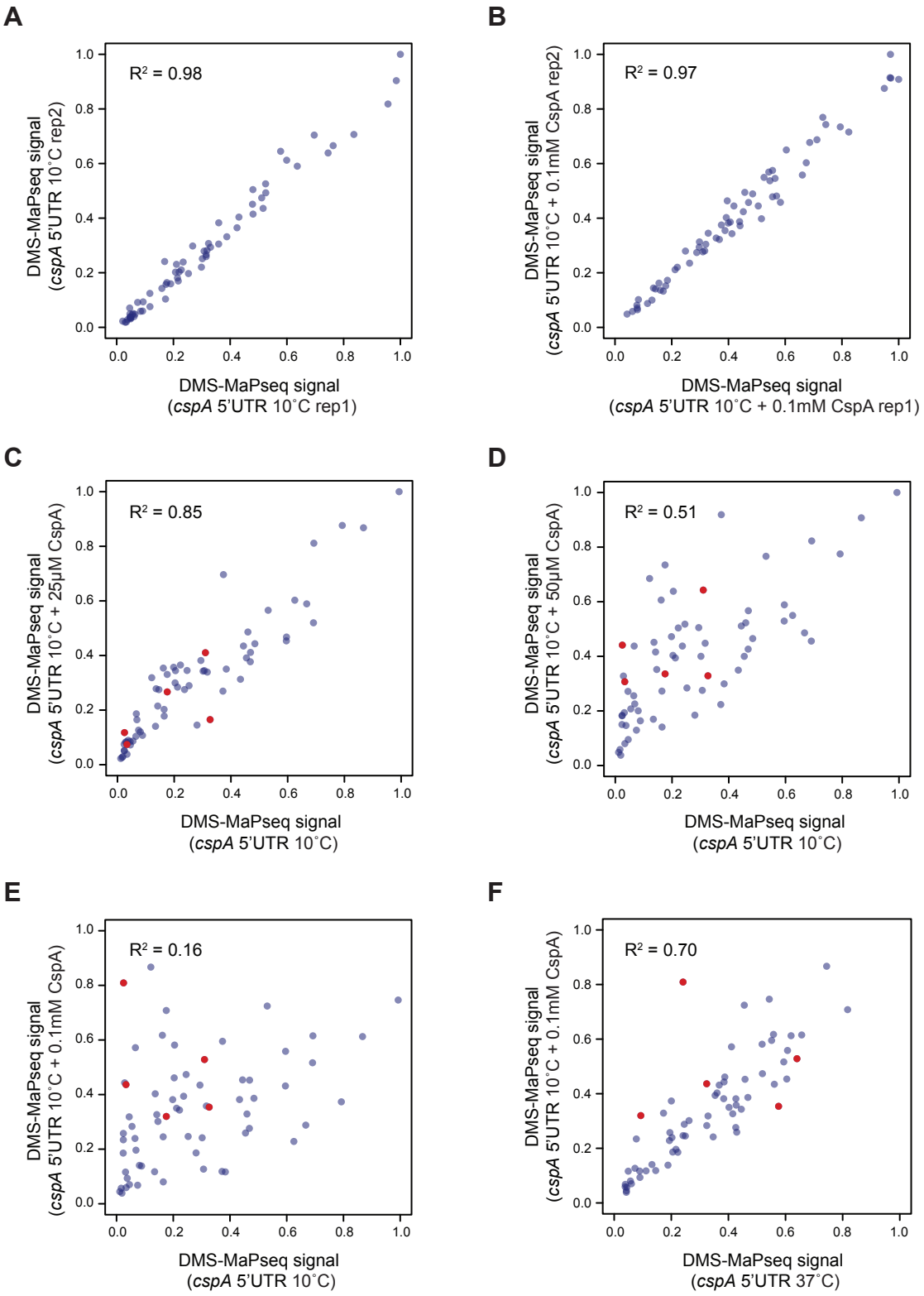
A
R² = 0.98
DMS-MaPseq signal (cspA 5'UTR 10˚C rep2)
DMS-MaPseq signal (cspA 5'UTR 10˚C rep1)
B
R² = 0.97
DMS-MaPseq signal (cspA 5'UTR 10˚C + 0.1mM CspA rep2)
DMS-MaPseq signal (cspA 5'UTR 10˚C + 0.1mM CspA rep1)
C
R² = 0.85
DMS-MaPseq signal (cspA 5'UTR 10˚C + 25μM CspA)
DMS-MaPseq signal (cspA 5'UTR 10˚C)
D
R² = 0.51
DMS-MaPseq signal (cspA 5'UTR 10˚C + 50μM CspA)
DMS-MaPseq signal (cspA 5'UTR 10˚C)
E
R² = 0.16
DMS-MaPseq signal (cspA 5'UTR 10˚C + 0.1mM CspA)
DMS-MaPseq signal (cspA 5'UTR 10˚C)
F
R² = 0.70
DMS-MaPseq signal (cspA 5'UTR 10˚C + 0.1mM CspA)
DMS-MaPseq signal (cspA 5'UTR 37˚C)

Figure S7, related to Figure 6: *In vitro* structural change of *cspA* 5'UTR by addition of CspA protein

(A-B) Scatter plot comparing *in vitro* DMS-MaPseq signal of A/C bases within *cspA* 5'UTR at 10°C (A) without CspA protein or (B) with 0.1mM CspA protein between two replicates. Pearson's correlation coefficient (R^2) was indicated. Signals are normalized to the most reactive position in the 5'UTR of *cspA.*

(C-E) Scatter plot comparing *in vitro* DMS-MaPseq signal of A/C bases within *cspA* 5'UTR at 10°C alone vs in the presence of (C) 25μM, (D) 50μM or (E) 0.1mM CspA protein. DMS-MaPseq data was first normalized to the most reactive position in the 5'UTR of *cspA.* Biological replicates of samples were adjusted by 90% percentile of signals and then averaged. Signals shown are mean values of adjusted replicates and error bars indicate standard deviation of 2-4 replicates. Red dots indicate signals at the A/C bases within the red regions (nt 113-118) in Figure 6A.

(F) Scatter plot comparing *in vitro* DMS-MaPseq signal of A/C bases within *cspA* 5'UTR at 37°C and the signals at 10°C with 0.1mM CspA protein. Signals are normalized as above. Red dots indicate signals at the A/C bases within the red regions (nt 113-118) in Figure 6A.